10th IFAC Symposium on Robot Control
International Federation of Automatic Control
September 5-7, 2012. Dubrovnik, Croatia

Dynamic Model and Control of an Over-actuated Quadrotor UAV

Riccardo Falconi * **Claudio Melchiorri** **

* *e-mail: riccardo.falconi@unibo.it*
** *e-mail: claudio.melchiorri@unibo.it.*

Abstract: In this paper, a novel omnidirectional unmanned flying vehicle (UAV) is presented. Staring from the well known quadrotor model, some features has been introduced in order to create an over-actuated quadrotor able to fly performing maneuvers that are typically not feasible for UAVs. An inverse dynamics control scheme is proposed to control the modified flying vehicle, with particular attention to the asset control. The stability and versatility of the solution has been proven by means of numerical simulations.

Keywords: Quadrotor, UAV, Inverse Dynamics Control.

1. INTRODUCTION

The development of Unmanned Aerial Vehicles (UAV) has attracted the attention of many researchers and industries due to their versatility and the relatively low cost of development and maintenance with respect to manned vehicles. Along with the increasing ability of creating more complex and miniaturized mechanisms, in past years UAVs have been used for a wide range of missions, both military and civilian. For example, UAVs were used in search and rescue missions in disaster areas (Quaritsch et al., 2010), in infrastructures and environmental monitoring (Morbidi et al., 2011; Metni and Hamel, 2007), and sensors deployment missions (Corke et al., 2004), for hazardous material handling (Maza et al., 2010) or for aerial surveillance (Grocholsky et al., 2006). Due to such different tasks, different UAV models has been proposed, mainly relying on two different designs: fixed wing UAV, whose main advantages are the long flying time and the low cost of maintenance, and rotary wing UAV, widely used due to their hovering ability and high maneuverability. Moreover, as long as the research was pushed toward the realization of small-size UAVs, new designs combining the above mentioned skills have been proposed in the literature. In particular, trying to develop mechanically simple flying vehicles, solutions based on multi rotor systems have been proposed. Beside new configurations exploiting a single propeller, such as the ducted fan UAVs (Marconi et al., 2006; Naldi et al., 2008; Gentili et al., 2008), alternative solutions exploiting configurations with more than one motor have been designed. In (Salazar-Cruz and Lozano, 2005; Yoo et al., 2010), a trirotor with two counter-rotating propellers and a tail adjustable motor has been presented. A tilt-wing quadrotor has been proposed in (Hancer et al., 2010) in order to combine the hovering skills of helicopters with the long range flying ability of the airplanes. This approach resulted so promising that it was adopted for a new class of military air carriers, namely the Bell Boeing V-22 Osprey actually used by the USAF and the forthcoming V-44 Osprey. Anyway, the most 'popular' UAV with multiple rotors is the quadrotor (Hoffmann et al., 2007; Cabecinhas et al., 2010), characterized by an extremely simple, reliable and low cost structure suitable for many applications. In recent years, the quadrotor concept has been used as the starting point to design much more complex UAVs, such as the six rotors (Yin et al., 2010) or eight rotors UAVs (Romero et al., 2007), whose main advantage compared to standard quadrotors is the improved stability despite the vehicle autonomy. Moreover, in order to improve the versatility of these vehicles, a number of tools such as cameras or small probes have been purposely developed.

Nevertheless, the main drawback of these devices is their intrinsic inability of an ideal holonomic flying capability. In fact, due to their mechanical structure, they cannot decouple translational and rotational movements. On the other hand, this capability would be useful in all those applications where the orientation of the UAV cannot be coupled with its flying direction. As an example, let us consider an activity such as infrastructure (bridge) inspection, sensors deploying or surveillance, where the possibility of adjusting the orientation of the vehicle without changing its flying direction would lead to better performances.

In this paper a novel quadrotor concept is proposed (Vivarelli, 2012). The quadrotor is designed to perform maneuvers as an holonomic device, thus decoupling translations and rotations movements. This goal is achieved by adding some actuators in order to change the directions of the forces applied by the rotors to the vehicle. This structure, to the best of the authors' knowledge, has never been proposed before in the literature. This paper is organized as follows. Sec. 2 presents the kinematic configuration and the main properties of the proposed device. Sect. 3 illustrates the dynamic model of the proposed vehicle, while Sec. 4 describes the control scheme, based on the well-known inverse dynamics approach. Sec. 5 reports some results obtained by simulations, showing the features and capabilities of the UAV, while Sec. 6 concludes with final comments and future work.

⋆ Riccardo Falconi and Claudio Melchiorri are with the Dipartimento di Elettronica, Informatica e Sistemistica of the Università di Bologna, Italy.

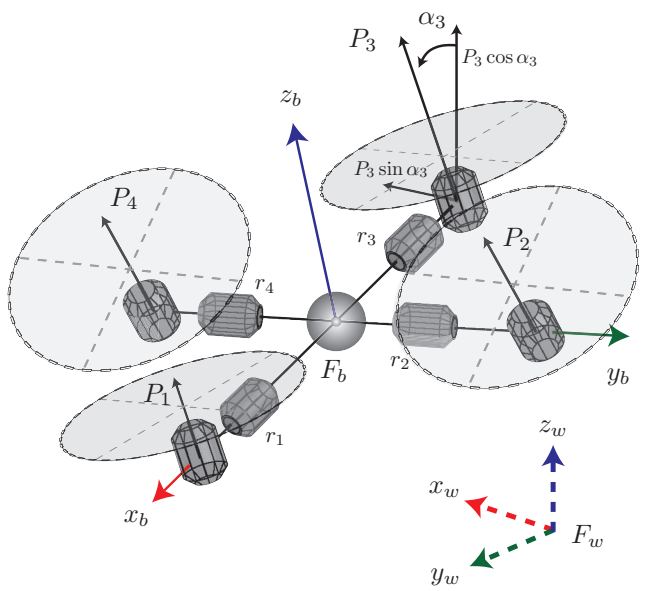

Fig. 1. Scheme of the modified quadrotor with the *pivoting* joints.

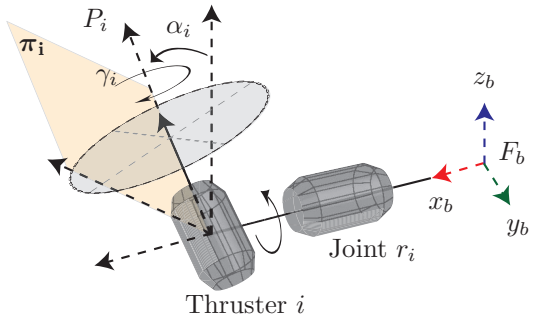

Fig. 2. Scheme of the actuated joint placed on the quadrotor's arms.

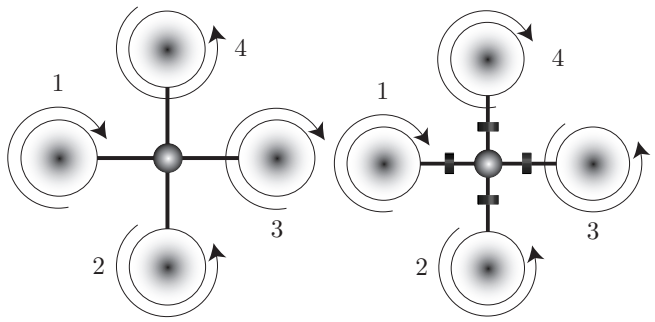

(a) Direction of rotation of the propellers in a standard quadrotor

(b) Direction of rotation of the propellers in the modified quadrotor

Fig. 3. Comparison between the direction of rotation of the propellers in a standard quadrotor model Fig. 3(a) and in the modified version Fig. 3(b).

2. THE PROPOSED QUADROTOR

In order to obtain an UAV able to fly decoupling linear and rotational movements, thus allowing operations that are not usually possible with standard flying vehicles, the proposed quadrotor has some structural differences with respect to standard devices.

The most important difference is shown in Fig. 1, where a scheme of the proposed quadrotor is reported. As it can be seen, an actuated rotational (*pivot*) joint r_i is installed on each arm of the vehicle, thus allowing to rotate the corresponding propeller by the angle α_i. In this manner, the force P_i generated by the propeller may be directed along any direction in a plane orthogonal to the corresponding arm (the plane π_i in Fig. 2).

Another difference with respect to a standard quadrotor is the rotating direction of the thrusters. In fact, as shown in Fig. 3(a), in a standard quadrotor the couple of propellers {1, 3} rotates clockwise, while propellers {2, 4} rotate counter-clockwise. This configuration ensures that, in hovering maneuvers, it is always possible to rotate the quadrotor about its z-axis by slowing down opposite propellers, but preserving the balance of the counteracting torques. In our case, as depicted in Fig. 3(b), we consider as rotating in the same direction the thrusters positioned at the opposite side of the quadrotor, e.g {1, 4} rotate clockwise and {2, 3} rotate counterclockwise.
This choice is motivated by the goal of increasing the maneuverability of the quadrotor with respect to classic models. In particular, considering the case that a rotation along the z-axis is required, the non compensated counteracting torques generated by the motors can be easily compensated by properly rotating the *pivot* motors. On the other hand, this configuration allows the UAV to translate by simply rotating two opposite propellers. Anyway, due to the redundancy of the proposed system (eight actuators), both configurations can be chosen for the propellers rotating directions.

3. THE DYNAMIC MODEL

In order to define the dynamic model of the quadrotor, an inertial reference frame F_w and a frame F_b rigidly connected with the quadrotor body are assigned. The axes x_b and y_b of F_b are directed along the arms connecting the body with propeller 1 and 2 respectively, while z_b is oriented to complete the frame, see Fig. 1.

For simplicity, the UAV is considered as a rigid body whose position and orientation with respect to F_w depends on the propulsion forces generated by the four rotors. Then, the dynamic model is obtained by applying the Newton-Euler equations of motion of a rigid body in the configuration space $SE(3) = \mathbb{R}^3 \times SO(3)$. Let $\boldsymbol{p} = [x,\ y,\ z]^T$ be the position of the center of mass of the quadrotor, and $\mathbf{R}$ the rotation matrix that describes its orientation, both expressed in F_w. Then, the dynamic model can be computed as

$$\begin{cases} m\ddot{\boldsymbol{p}} = \boldsymbol{R}\boldsymbol{f}_b + m\boldsymbol{g} \\ \boldsymbol{J}\dot{\boldsymbol{\omega}} = -\boldsymbol{\omega}^{\times}\boldsymbol{J}\boldsymbol{\omega} + \boldsymbol{\tau}_b \end{cases} \tag{1}$$

where $\boldsymbol{J} = \mathrm{diag}([J_x,\ J_y,\ J_z])$ is the inertia diagonal matrix expressed in the body reference frame, m is the total mass of the vehicle, $\boldsymbol{g} = [0,\ 0,\ -g]^T$ (with $g = 9.81$ [m/s^2]) is the gravity acceleration vector, while $\boldsymbol{f}_b$, $\boldsymbol{\tau}_b$ are respectively the overall forces and torques applied to the quadrotor, expressed in the body reference frame. The superscript $^{\times}$ in Eq. (1) addresses the *skew* operator, i.e. if $\mathbf{s} = [s_1,\ s_2,\ s_3]^T$, then $\boldsymbol{s}^{\times}$ is the skew-symmetric matrix

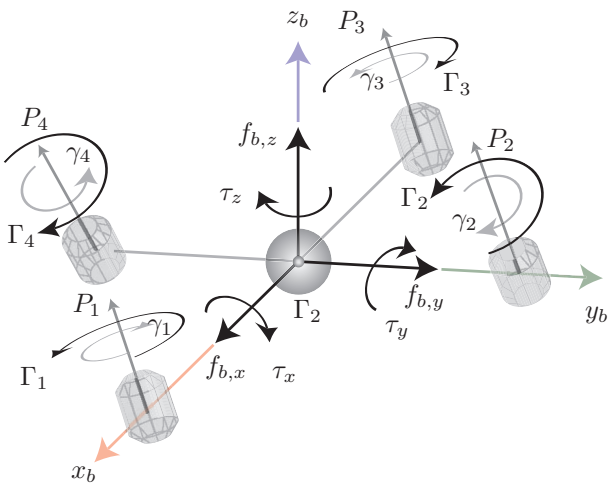

Fig. 4. Force and torque generated by the propellers on the body frame of the quadrotor.

$$\boldsymbol{s}^{\times} = \begin{bmatrix} 0 & -s_3 & s_2 \\ s_3 & 0 & -s_1 \\ -s_2 & s_1 & 0 \end{bmatrix} \tag{2}$$

Since it is of interest to show the potentiality of the new quadrotor and not to analyze in detail the physical properties of the model, second order effects related to aerodynamics effects, such as the propellers flapping or the gyroscopic precession torques due to the angular speed of the propellers (Hoffmann et al., 2007), (Prouty, 2001), or due to the actuators dynamics, have been neglected.

By defining as γ_i (> 0) the rotation velocity of the i-th propeller, and with α_i the orientation of the i-th pivot joint (see Fig. 2), the terms $\boldsymbol{f}_b$ and $\boldsymbol{\tau}_b$ in Eq. (1) can be defined by considering that the corresponding propeller affects the dynamics of the quadrotor in two ways: by generating a propulsion force P_i orthogonal to the propeller itself, and by generating a counteracting torque Γ_i (see Fig. 4). In particular, as described in (Pounds et al., 2010), it is possible to consider these two contributions as:

$$P_i = k_{f,i}\gamma_i^2 \tag{3}$$

$$\Gamma_i = k_{\tau,i}\gamma_i^2 + I_{r,i}\dot{\gamma}_i \tag{4}$$

where $I_{r,i}$ is the motor inertia and $k_{f,i}, k_{\tau,i}$ are two parameters that depend on the air density and on geometrical properties of the i-th propeller (see (Pounds et al., 2010)).

The term $\boldsymbol{f}_b = [f_{b,x},\ f_{b,y},\ f_{b,z}]^T$ in Eq. (1) represents the forces generated by the propellers on the quadrotor body. By considering the model in Fig. 1, it can be calculated as:

$$\begin{aligned} \begin{bmatrix} f_{b,x} \\ f_{b,y} \\ f_{b,z} \end{bmatrix} &= \begin{bmatrix} P_2 S_{\alpha_2} - P_4 S_{\alpha_4} \\ P_3 S_{\alpha_3} - P_1 S_{\alpha_1} \\ P_1 C_{\alpha_1} + P_2 C_{\alpha_2} + P_3 C_{\alpha_3} + P_4 C_{\alpha_4} \end{bmatrix} \\ &= \begin{bmatrix} 0 & S_{\alpha_2} & 0 & -S_{\alpha_4} \\ -S_{\alpha_1} & 0 & S_{\alpha_3} & 0 \\ C_{\alpha_1} & C_{\alpha_2} & C_{\alpha_3} & C_{\alpha_4} \end{bmatrix} \boldsymbol{P} \\ &= \boldsymbol{B}_f \cdot \boldsymbol{P} \end{aligned} \tag{5}$$

where $\boldsymbol{P} = [P_1,\ P_2,\ P_3,\ P_4]^T$ is the vector collecting the thrusts generated by the four propellers, and $S_{\alpha_i} = \sin(\alpha_i)$, $C_{\alpha_i} = \cos(\alpha_i)$.

The term $\boldsymbol{\tau}_b$ in Eq. (1) can be written as the sum of two contributions, namely

$$\boldsymbol{\tau}_b = \boldsymbol{\tau}_m + \boldsymbol{\tau}_c \tag{6}$$

where $\boldsymbol{\tau}_m$ and $\boldsymbol{\tau}_c$ represent the momenta generated by the forces $\boldsymbol{P}$ on the body frame and the counteracting torques generated by the rotors, respectively. Assuming for simplicity that the arms of the quadrotor have the same length ℓ, $\boldsymbol{\tau}_m = [\tau_{m,x},\ \tau_{m,y},\ \tau_{m,z}]^T$ can be calculated as

$$\begin{aligned} \begin{bmatrix} \tau_{m,x} \\ \tau_{m,y} \\ \tau_{m,z} \end{bmatrix} &= \ell \begin{bmatrix} P_2 C_{\alpha_2} - P_4 C_{\alpha_4} \\ P_3 C_{\alpha_3} - P_1 C_{\alpha_1} \\ -P_1 S_{\alpha_1} - P_2 S_{\alpha_2} - P_3 S_{\alpha_3} - P_4 S_{\alpha_4} \end{bmatrix} = \\ &= \ell \begin{bmatrix} 0 & C_{\alpha_2} & 0 & -C_{\alpha_4} \\ -C_{\alpha_1} & 0 & C_{\alpha_3} & 0 \\ -S_{\alpha_1} & -S_{\alpha_2} & -S_{\alpha_3} & -S_{\alpha_4} \end{bmatrix} \boldsymbol{P} = \\ &= \ell\, \boldsymbol{B}_m\, \boldsymbol{P} \end{aligned} \tag{7}$$

By considering the definition of Γ_i given in Eq. (4), the term $\boldsymbol{\tau}_c = [\tau_{c,x},\ \tau_{c,y},\ \tau_{c,z}]^T$ can be written as

$$\begin{aligned} \begin{bmatrix} \tau_{c,x} \\ \tau_{c,y} \\ \tau_{c,z} \end{bmatrix} &= \begin{bmatrix} \Gamma_4 S_{\alpha_4} - \Gamma_2 S_{\alpha_2} \\ \Gamma_3 S_{\alpha_3} - \Gamma_1 S_{\alpha_1} \\ \Gamma_1 C_{\alpha_1} - \Gamma_2 C_{\alpha_2} + \Gamma_3 C_{\alpha_3} - \Gamma_4 C_{\alpha_4} \end{bmatrix} = \\ &= \begin{bmatrix} 0 & -S_{\alpha_2} & 0 & S_{\alpha_4} \\ -S_{\alpha_1} & 0 & S_{\alpha_3} & 0 \\ C_{\alpha_1} & -C_{\alpha_2} & C_{\alpha_3} & -C_{\alpha_4} \end{bmatrix} \boldsymbol{\Gamma} = \\ &= \boldsymbol{B}_c \boldsymbol{\Gamma} \end{aligned} \tag{8}$$

where $\boldsymbol{\Gamma} = [\Gamma_1,\ \Gamma_2,\ \Gamma_3,\ \Gamma_4]^T$ is the vector collecting all the counteracting torques generated by the rotating propellers. By defining $\hat{k}_i = \dfrac{k_{f,i}}{k_{\tau,i}}$, the counteracting torque Γ_i in Eq. (4) can be rewritten as $\Gamma_i = \hat{k}_i P_i + I_{r,i}\dot{\gamma}_i$, or, in a matrix form, as

$$\boldsymbol{\Gamma} = \hat{\boldsymbol{K}}\boldsymbol{P} + \boldsymbol{I}_r\dot{\boldsymbol{\gamma}} \tag{9}$$

where

$$\hat{\boldsymbol{K}} = \begin{bmatrix} \hat{k}_1 & 0 & 0 & 0 \\ 0 & \hat{k}_2 & 0 & 0 \\ 0 & 0 & \hat{k}_3 & 0 \\ 0 & 0 & 0 & \hat{k}_4 \end{bmatrix} \quad \hat{\boldsymbol{I}}_r = \begin{bmatrix} I_{r,1} & 0 & 0 & 0 \\ 0 & I_{r,2} & 0 & 0 \\ 0 & 0 & I_{r,3} & 0 \\ 0 & 0 & 0 & I_{r,4} \end{bmatrix}$$

By exploiting Eq. (9), the vector $\boldsymbol{\tau}_c$ in Eq. (8) becomes

$$\boldsymbol{\tau}_c = \boldsymbol{B}_c(\hat{\boldsymbol{K}}\boldsymbol{P} + \hat{\boldsymbol{I}}_r\dot{\boldsymbol{\gamma}}) \tag{10}$$

Finally, from Eq. (5), (7) and (10), the dynamic model of the quadrotor in (1) becomes

$$\begin{cases} m\ddot{\boldsymbol{p}} = \boldsymbol{R}\boldsymbol{B}_f\boldsymbol{P} + m\boldsymbol{g} \\ \boldsymbol{J}\dot{\boldsymbol{\omega}} = -\boldsymbol{\omega}^{\times}\boldsymbol{J}\boldsymbol{\omega} + \left(\ell\boldsymbol{B}_m + \boldsymbol{B}_c\hat{\boldsymbol{K}}\right)\boldsymbol{P} + \boldsymbol{B}_c\hat{\boldsymbol{I}}_r\dot{\boldsymbol{\gamma}} \end{cases} \tag{11}$$

4. INVERSE DYNAMICS CONTROL

For control purposes, and in particular for avoiding discontinuities in the angular representation (a typical problem arising when the *Euler* or the *Roll*, *Pitch* and *Yaw* angles are used to define the pose of a rigid body in space), the unit quaternion representation is adopted here for defining the angular pose of the UAV, (Chaturvedi et al., 2011). As it is well known, a unit quaternion expressed in a given frame F is a four dimensional vector $\boldsymbol{q} = (q_0, \boldsymbol{\eta}) \in \mathbb{R}^4$,

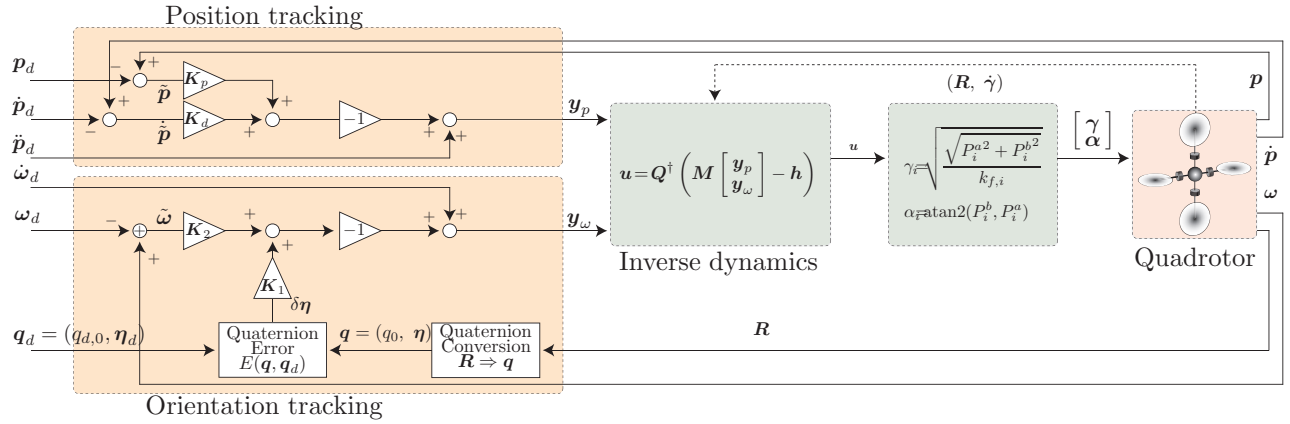

Fig. 5. Inverse dynamics control scheme for the proposed quadrotor.

where q_0 denotes the scalar part of the quaternion and $\boldsymbol{\eta} = [q_1,\ q_2,\ q_3]^T$ denotes its vectorial part. Moreover

$$\boldsymbol{q} = q_0 + q_1\hat{i} + q_2\hat{j} + q_3\hat{k}$$

with the constraint $q_0^2 + q_1^2 + q_2^2 + q_3^2 = 1$; $\hat{i}, \hat{j}, \hat{k}$ are the unit vectors of the x, y, z axes of frame F. Given a rotation matrix $\boldsymbol{R} = [R_{ij}]$ that describes the asset of the body frame F_b with respect to the inertial frame F_w, the corresponding quaternion can be computed as:

$$\begin{aligned} q_0 &= \frac{1}{2}\sqrt{1 + R_{11} + R_{22} + R_{33}}, & q_1 &= \frac{R_{32} - R_{23}}{4q_0} \\ q_2 &= \frac{R_{13} - R_{31}}{4q_0}, & q_3 &= \frac{R_{21} - R_{12}}{4q_0} \end{aligned} \tag{12}$$

The derivative of the quaternion vector is calculated using the *quaternion propagation rule*, namely $\dot{\boldsymbol{q}} = (\dot{q_0}, \dot{\boldsymbol{\eta}})$ with

$$\dot{q}_0 = -\frac{1}{2}\hat{\boldsymbol{q}}^T\boldsymbol{\omega} \qquad \dot{\boldsymbol{\eta}} = \frac{1}{2}\left[q_0\boldsymbol{I}_3 + \boldsymbol{\eta}^{\times}\right]\boldsymbol{\omega} \tag{13}$$

being $\boldsymbol{I}_3$ is the 3×3 identity matrix. Further discussions on quaternion properties and on the quaternion propagation rule can be found e.g. in (Nikravesh et al., 1985; Caccavale and Villani, 1999).

Given two generic quaternions $\boldsymbol{a} = (a_0,\ \boldsymbol{\eta}_a)$ and $\boldsymbol{b} = (b_0,\ \boldsymbol{\eta}_b)$, the relative difference (error) $\delta\boldsymbol{q} = (\delta q_0,\ \delta\boldsymbol{\eta})$ is defined as:

$$\delta\boldsymbol{q} = \begin{bmatrix} \delta q_0 \\ \delta\boldsymbol{\eta} \end{bmatrix} = \begin{bmatrix} a_0 & -\boldsymbol{\eta}_a^T \\ \boldsymbol{\eta}_a & a_0\boldsymbol{I}_3 + \boldsymbol{\eta}_a^{\times} \end{bmatrix}\begin{bmatrix} b_0 \\ -\boldsymbol{\eta}_b \end{bmatrix} = E(\boldsymbol{a}, \boldsymbol{b}) \tag{14}$$

The basic idea of the inverse dynamics control scheme is to define a non linear control law able to cancel the nonlinearities and couplings of the controlled plant, thus creating a closed loop system ideally linear and decoupled, (de Wit et al., 1996). For this purpose, notice that the thrust of the i-th propeller may be decomposed into two contributions, namely:

$$P_i^a = P_i\cos\alpha_i, \qquad P_i^b = P_i\sin\alpha_i \tag{15}$$

from which it follows that $\alpha_i = \text{atan2}(P_i^b, P_i^a)$. By defining the input vector $\boldsymbol{u}$ as

$$\boldsymbol{u} = \left[P_1^a,\ P_1^b,\ P_2^a,\ P_2^b,\ P_3^a,\ P_3^b,\ P_4^a,\ P_4^b\ \right]^T \tag{16}$$

the vectors $\boldsymbol{B}_f\boldsymbol{P}$, $\boldsymbol{B}_m\boldsymbol{P}$ and $\boldsymbol{B}_c\boldsymbol{P}$ can be written as:

$$\begin{aligned} \boldsymbol{B}_f\boldsymbol{P} &= \underbrace{\begin{bmatrix} 0 & 0 & 0 & 1 & 0 & 0 & 0 & -1 \\ 0 & -1 & 0 & 0 & 0 & 1 & 0 & 0 \\ 1 & 0 & 1 & 0 & 1 & 0 & 1 & 0 \end{bmatrix}}_{\boldsymbol{A}_f}\boldsymbol{u} \\ \ell\boldsymbol{B}_m\boldsymbol{P} &= \underbrace{\ell\begin{bmatrix} 0 & 0 & 1 & 0 & 0 & 0 & -1 & 0 \\ -1 & 0 & 0 & 0 & 1 & 0 & 0 & 0 \\ 0 & -1 & 0 & -1 & 0 & -1 & 0 & -1 \end{bmatrix}}_{\boldsymbol{A}_m}\boldsymbol{u} \\ \boldsymbol{B}_c\hat{\boldsymbol{K}}\boldsymbol{P} &= \underbrace{\begin{bmatrix} 0 & 0 & 0 & -\hat{k}_2 & 0 & 0 & 0 & \hat{k}_4 \\ 0 & -\hat{k}_1 & 0 & 0 & 0 & \hat{k}_3 & 0 & 0 \\ \hat{k}_1 & 0 & -\hat{k}_2 & 0 & \hat{k}_3 & 0 & -\hat{k}_4 & 0 \end{bmatrix}}_{\boldsymbol{A}_c}\boldsymbol{u} \end{aligned}$$

Then, the dynamic model can be rewritten as

$$\begin{cases} m\ddot{\boldsymbol{p}} = \boldsymbol{R}\boldsymbol{A}_f\boldsymbol{u} + m\boldsymbol{g} \\ \boldsymbol{J}\dot{\boldsymbol{\omega}} = (\boldsymbol{A}_m + \boldsymbol{A}_c)\,\boldsymbol{u} + \boldsymbol{t} \end{cases} \tag{17}$$

where $\boldsymbol{t} = -\boldsymbol{\omega}^{\times}\boldsymbol{J}\boldsymbol{\omega} + \boldsymbol{B}_c\hat{\boldsymbol{I}}_r\dot{\boldsymbol{\gamma}}$. By defining the matrices $\boldsymbol{M}$, $\boldsymbol{Q}$ and the vector $\boldsymbol{h}$ as

$$\boldsymbol{M} = \begin{bmatrix} m\,\boldsymbol{I}_3 & \boldsymbol{0}_3 \\ \boldsymbol{0}_3 & \boldsymbol{J} \end{bmatrix},\ \boldsymbol{Q} = \begin{bmatrix} \boldsymbol{R}\boldsymbol{A}_f \\ \boldsymbol{A}_m + \boldsymbol{A}_c \end{bmatrix},\ \boldsymbol{h} = \begin{bmatrix} m\boldsymbol{g} \\ \boldsymbol{t} \end{bmatrix}$$

being $\boldsymbol{0}_3$ the 3×3 null matrix, the dynamic model (17) becomes

$$\boldsymbol{M}\begin{bmatrix} \ddot{\boldsymbol{p}} \\ \dot{\boldsymbol{\omega}} \end{bmatrix} = \boldsymbol{Q}\boldsymbol{u} + \boldsymbol{h} \tag{18}$$

Now, by choosing $\boldsymbol{u} = \boldsymbol{Q}^{\dagger}\left(\boldsymbol{M}\begin{bmatrix} \boldsymbol{y}_p \\ \boldsymbol{y}_\omega \end{bmatrix} - \boldsymbol{h}\right)$, it follows that

$$\begin{bmatrix} \ddot{\boldsymbol{p}} \\ \dot{\boldsymbol{\omega}} \end{bmatrix} = \begin{bmatrix} \boldsymbol{y}_p \\ \boldsymbol{y}_\omega \end{bmatrix}$$

where $\boldsymbol{Q}^{\dagger}$ is the *Moore-Penrose* pseudoinverse of $\boldsymbol{Q}$ (Moore, 1920)and $\boldsymbol{y}_p$, $\boldsymbol{y}_\omega$ two new control actions to be properly defined for stability and tracking purposes.

Assuming that a desired trajectory is provided in terms of position $\{\boldsymbol{p}_d,\ \dot{\boldsymbol{p}}_d,\ \ddot{\boldsymbol{p}}_d\}$ and orientation $\{\boldsymbol{q}_d,\ \boldsymbol{\omega}_d, \dot{\boldsymbol{\omega}}_d\}$, it is possible to define for the position tracking the following PD with feedforward control input:

$$\boldsymbol{y}_p = \ddot{\boldsymbol{p}}_d - \boldsymbol{K}_d\dot{\tilde{\boldsymbol{p}}} - \boldsymbol{K}_p\tilde{\boldsymbol{p}} \tag{19}$$

where $\boldsymbol{K}_p > 0$, $\boldsymbol{K}_d > 0$ are two diagonal positive definite matrices, $\tilde{\boldsymbol{p}} = \boldsymbol{p} - \boldsymbol{p}_d$ and $\dot{\tilde{\boldsymbol{p}}} = \dot{\boldsymbol{p}} - \dot{\boldsymbol{p}}_d$ are the position and velocity error respectively.

Parameter	*Description*	*Value*	*Units*
Gravity	g	9.81	$[m/s^2]$
Quadrotor radius	ℓ	0.225	$[m]$
Mass	m	0.468	$[Kg]$
Inertia matrix	$J_x = J_y = J_z$	$4.9 \cdot 10^{-3}$	$[Kg \cdot m^2]$
Rotor inertia	$I_{r,i}$	$3.4 \cdot 10^{-5}$	$[Kg \cdot m^2]$
Propellers coefficients	$k_{f,i}$	$2.9 \cdot 10^{-5}$	
Rotor coupling coeff.	$k_{c,i}$	$1.1 \cdot 10^{-6}$	

Table 1. Nominal physical parameters used in simulations.

With regard to the asset control, it is possible to define a quaternion based controller as

$$\boldsymbol{y}_\omega = \dot{\boldsymbol{\omega}}_d - \boldsymbol{K}_2\tilde{\boldsymbol{\omega}} - \boldsymbol{K}_1\delta\boldsymbol{\eta} \tag{20}$$

where $\boldsymbol{K}_1 > 0$, $\boldsymbol{K}_2 > 0$ two diagonal positive definite matrices, $\tilde{\boldsymbol{\omega}} = (\boldsymbol{\omega} - \boldsymbol{\omega}_d)$ is the angular velocity error, and $\delta\boldsymbol{\eta}$ is the vector part of $E(\boldsymbol{q}, \boldsymbol{q}_d)$, (14), where $\boldsymbol{q}_d$ is the quaternion describing the desired orientation of the quadrotor. The stability properties of these control actions can be easily shown by a Lyapunov-based demonstration, as reported e.g. in (Chaturvedi et al., 2011). The overall control scheme is reported in Fig. 5.

Notice that, due to the proposed mechanical configuration of the quadrotor, it is possible to exploit the redundancy of the system in order to modify the computation of the pseudoinverse of the matrix $\boldsymbol{Q}$ to define an optimal control able to minimize a given cost function (Athans and Falb, 2006), or, alternatively, to create more complex behaviors by using e.g. the *null space behavioral* approach, (Antonelli et al., 2008). However, because of its definition, the *Moore-Penrose* pseudoinverse already minimizes the energy used by the system to track the given trajectory. Finally, note that it is possible to adopt robust control techniques if the parameters of the dynamic model are not perfectly known.

5. SIMULATIONS

The dynamic model of the quadrotor presented in this paper has been implemented in Matlab/Simulink, with the inverse dynamics controller described in the previous section. In the simulations, the actuators generating the velocities $\boldsymbol{\gamma}$ and modifying the angle $\boldsymbol{\alpha}$ have been modeled as first-order filters with unit gain with proper time-constants. Some results are now illustrated to highlight the performances of the proposed UAV, in particular focusing on maneuvers that cannot be performed by standard quadrotors (and also by almost all other flying vehicles).

The test trajectory provided to the controller of the quadrotor is shown in Fig. 6. The desired position and orientation are shown in Fig. 6(a) and Fig. 6(b) respectively. In particular note that, even if both the dynamic model and the controller make use of the quaternion representation for the vehicle asset, for the sake of clarity the desired orientation is expressed with Euler angles.

The physical parameters used in the simulations are reported in Table 1. These parameters are compatible with those of the quadrotor in (Tayebi and McGilvray, 2006), one of the most common in research activities. Notice that, from the data-sheet provided by manufacturer, this quadrotor has a payload that, with some modifications, allows to use the same frame to create the proposed UAV,

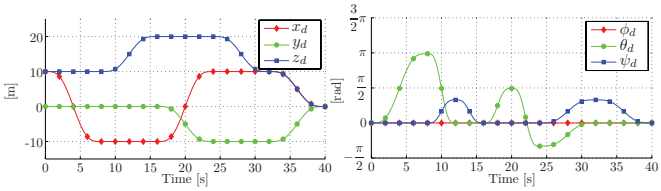

(a) Position trajectory. (b) Euler angles of the desired trajectory.

Fig. 6. Position Fig. 6(a) and orientation Fig. 6(b) plots of the desired trajectory.

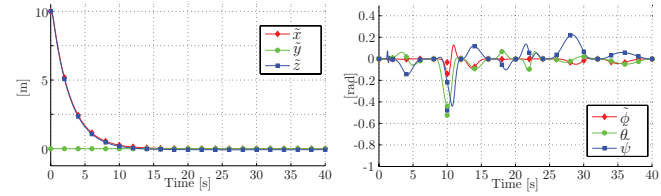

(a) Position tracking error, with $\tilde{x} = x_d - x$, $\tilde{y} = y_d - y$, $\tilde{z} = z_d - z$. (b) Asset error in terms of *Euler angles*, with $\tilde{\phi} = \phi_d - \phi$, $\tilde{\theta} = \theta_d - \theta$, $\tilde{\psi} = \psi_d - \psi$.

Fig. 7. Position an orientation errors tracking the trajectory in Fig. 6.

at least preserving the same body dimensions and the same thrusters and propellers. The control parameters are:

$$\begin{cases} K_p = 3300\ \boldsymbol{I}_3 \\ K_d = 92\ \boldsymbol{I}_3 \end{cases} \quad \begin{cases} K_1 = 33\ \boldsymbol{I}_3 \\ K_2 = 9.2\ \boldsymbol{I}_3 \end{cases}$$

The tracking errors are reported in Fig. 7.

6. CONCLUSIONS

In this paper, a novel unmanned flying vehicle able to achieve omnidirectional and decoupled motions has been presented. In particular, starting from the standard quadrotor model, an additional actuated rotational joint has been mounted in each arm of the vehicle, thus adding four new degrees of freedom. These additional joints allow to rotate the four thrusters independently, and can be exploited to redirect the forces generated by the propellers. After calculating the dynamic model of the proposed over-actuated quadrotor, an inverse dynamics controller has been defined, with particular attention to the problem of singularity representations in orientation.

The dynamic model and the proposed control algorithm have been verified by means of simulations in Matlab/Simulink, both considering the case of nominal conditions and the case of external disturbances. In both cases the results are quite satisfactory. In conclusion, the proposed quadrotor is able to perform maneuvers non possible to other vehicles, and this is achieved with a modest increase of the mechanical complexity. Current research activity aims at the definition of a more complete dynamic model, considering second order dynamic effects and the dynamics of the motors. Moreover, a laboratory prototype of this quadrotor is under definition and will be experimentally validated in the future.

REFERENCES

Antonelli, G., Arrichiello, F., and Chiaverini, S. (2008). The null-space-based behavioral control for

autonomous robotic systems. *Intelligent Service Robotics*, 1, 27–39. URL http://dx.doi.org/10.1007/s11370-007-0002-3. 10.1007/s11370-007-0002-3.

Athans, M. and Falb, P. (2006). *Optimal Control: An Introduction to the Theory and Its Applications*. Dover Books on Engineering Series. Dover Publications. URL http://books.google.com/books?id=7iocAgAACAAJ.

Cabecinhas, D., Naldi, R., Marconi, L., Silvestre, C., and Cunha, R. (2010). Robust take-off and landing for a quadrotor vehicle. In *Robotics and Automation (ICRA), 2010 IEEE International Conference on*, 1630 –1635. doi:10.1109/ROBOT.2010.5509430.

Caccavale, F. and Villani, L. (1999). Output feedback control for attitude tracking. *Systems & Control Letters*, 38(2), 91 – 98. doi:DOI:10.1016/S0167-6911(99)00050-X. URL http://www.sciencedirect.com/science/article/pii/S016769119900050X.

Chaturvedi, N., Sanyal, A., and McClamroch, N. (2011). Rigid-body attitude control. *Control Systems, IEEE*, 31(3), 30 –51. doi:10.1109/MCS.2011.940459.

Corke, P., Hrabar, S., Peterson, R., Rus, D., Saripalli, S., and Sukhatme, G. (2004). Autonomous deployment and repair of a sensor network using an unmanned aerial vehicle. In *Robotics and Automation, 2004. Proceedings. ICRA '04. 2004 IEEE International Conference on*, volume 4, 3602 – 3608 Vol.4. doi:10.1109/ROBOT.2004.1308811.

de Wit, C.C., Bastin, G., and Siciliano, B. (eds.) (1996). *Theory of Robot Control*. Springer-Verlag New York, Inc., Secaucus, NJ, USA, 1st edition.

Gentili, L., Naldi, R., and Marconi, L. (2008). Modeling and control of vtol uavs interacting with the environment. In *Decision and Control, 2008. CDC 2008. 47th IEEE Conference on*, 1231 –1236. doi:10.1109/CDC.2008.4739377.

Grocholsky, B., Keller, J., Kumar, V., and Pappas, G. (2006). Cooperative air and ground surveillance. *Robotics Automation Magazine, IEEE*, 13(3), 16 –25. doi:10.1109/MRA.2006.1678135.

Hancer, C., Oner, K., Sirimoglu, E., Cetinsoy, E., and Unel, M. (2010). Robust position control of a tilt-wing quadrotor. In *Decision and Control (CDC), 2010 49th IEEE Conference on*, 4908 –4913. doi:10.1109/CDC.2010.5717283.

Hoffmann, G.M., Huang, H., Wasl, S.L., and Tomlin, E.C.J. (2007). Quadrotor helicopter flight dynamics and control: Theory and experiment. In *In Proc. of the AIAA Guidance, Navigation, and Control Conference*.

Marconi, L., Naldi, R., and Sala, A. (2006). Modeling and analysis of a reduced-complexity ducted mav. In *Control and Automation, 2006. MED '06. 14th Mediterranean Conference on*, 1 –5. doi:10.1109/MED.2006.328770.

Maza, I., Kondak, K., Bernard, M., and Ollero, A. (2010). Multi-uav cooperation and control for load transportation and deployment. *Journal of Intelligent & Robotic Systems*, 57, 417–449. URL http://dx.doi.org/10.1007/s10846-009-9352-8. 10.1007/s10846-009-9352-8.

Metni, N. and Hamel, T. (2007). A UAV for bridge inspection: Visual servoing control law with orientation limits. *Automation in Construction*, 17(1), 3–10. doi:10.1016/j.autcon.2006.12.010. URL http://dx.doi.org/10.1016/j.autcon.2006.12.010.

Moore, E.H. (1920). On the reciprocal of the general algebraic matrix. *Bulletin of the American Mathematical Society*, 26, 394–395.

Morbidi, F., Freeman, R.A., and Lynch, K.M. (2011). Estimation and control of uav swarms for distributed monitoring tasks. In *American Control Conference (ACC), 2011*, 1069 –1075.

Naldi, R., Marconi, L., and Sala, A. (2008). Modelling and control of a miniature ducted-fan in fast forward flight. In *American Control Conference, 2008*, 2552 –2557. doi:10.1109/ACC.2008.4586875.

Nikravesh, P.E., Wehage, R.A., and Kwon, O.K. (1985). Euler parameters in computational kinematics and dynamics - part 1. *Journal of Mechanisms, Trasmissions, and Automation in Design*, 107, 358–365.

Pounds, P., Mahony, R., and Corke, P. (2010). Modelling and control of a large quadrotor robot. *Control Engineering Practice*, 18(7), 691 – 699. doi:DOI:10.1016/j.conengprac.2010.02.008. URL http://www.sciencedirect.com/science/article/pii/S0967066110000456. Special Issue on Aerial Robotics.

Prouty, R.W. (2001). *Helicopter Performance, Stability, and Control*. Krieger Pub Co. URL http://www.amazon.fr/exec/obidos/ASIN/1575242095/citeulike04-21.

Quaritsch, M., Kruggl, K., Wischounig-Strucl, D., Bhattacharya, S., Shah, M., and Rinner, B. (2010). Networked uavs as aerial sensor network for disaster management applications. *e & i Elektrotechnik und Informationstechnik*, 127, 56–63. URL http://dx.doi.org/10.1007/s00502-010-0717-2. 10.1007/s00502-010-0717-2.

Romero, H., Salazar, S., Sanchez, A., and Lozano, R. (2007). A new uav configuration having eight rotors: Dynamical model and real-time control. In *Decision and Control, 2007 46th IEEE Conference on*, 6418 –6423. doi:10.1109/CDC.2007.4434776.

Salazar-Cruz, S. and Lozano, R. (2005). Stabilization and nonlinear control for a novel trirotor mini-aircraft. In *Robotics and Automation, 2005. ICRA 2005. Proceedings of the 2005 IEEE International Conference on*, 2612 – 2617. doi:10.1109/ROBOT.2005.1570507.

Tayebi, A. and McGilvray, S. (2006). Attitude stabilization of a vtol quadrotor aircraft. *Control Systems Technology, IEEE Transactions on*, 14(3), 562 – 571. doi:10.1109/TCST.2006.872519.

Vivarelli, L. (2012). *Modellazione Dinamica e Simulazione di un Quadcopter Sovra-attuato.* Bachelor's thesis, Department of Electrical, Computer Science and Systems Engineering (DEIS), University of Bologna, Bologna, Italy.

Yin, L., Shi, J., and Huang, Y. (2010). Modeling and control for a six-rotor aerial vehicle. In *Electrical and Control Engineering (ICECE), 2010 International Conference on*, 1289 –1292. doi:10.1109/iCECE.2010.320.

Yoo, D.W., Oh, H.D., Won, D.Y., and Tahk, M.J. (2010). Dynamic modeling and control system design for tri-rotor uav. In *Systems and Control in Aeronautics and Astronautics (ISSCAA), 2010 3rd International Symposium on*, 762 –767. doi:10.1109/ISSCAA.2010.5632868.